A posteriori superlinear convergence bounds for block conjugate gradient

Christian E. Schaerer, Daniel B. Szyld,
and Pedro J. Torres

Report 21-07-11
July 2021

Department of Mathematics
Temple University
Philadelphia, PA 19122

This report is available in the World Wide Web at
`http://www.math.temple.edu/~szyld`

A POSTERIORI SUPERLINEAR CONVERGENCE BOUNDS FOR BLOCK CONJUGATE GRADIENT*

CHRISTIAN E. SCHAERER†, DANIEL B. SZYLD‡, AND PEDRO J. TORRES†

Abstract. In this paper, we extend to the block case, the *a posteriori* bound showing superlinear convergence of Conjugate Gradients developed in [J. Comput. Applied Math., 48 (1993), pp. 327-341], that is, we obtain similar bounds, but now for block Conjugate Gradients. We also present a series of computational experiments, illustrating the validity of the bound developed here, as well as the bound from [SIAM Review, 47 (2005), pp. 247272] using angles between subspaces. Using these bounds, we make some observations on the onset of superlinearity, and how this onset depends on the eigenvalue distribution and the block size.

Key words. superlinear convergence, block conjugate gradient method, *a posteriori* analysis.

AMS subject classifications. 65F10, 65B99, 65F30

1. Introduction.

The block conjugate gradient (block CG) is a generalization of the CG method [10] and was introduced by O'Leary in 1980 for solving systems with multiple right hand sides (rhs) simultaneously [13]. Given a real symmetric positive definite (s.p.d.) $n \times n$ matrix A and real $n \times s$ skinny-tall matrices (block vectors) $\mathbf{X}$ and $\mathbf{B}$, $s \ll n$; then the system

$$A\mathbf{X} = \mathbf{B} \tag{1}$$

is solved by block CG method in exact arithmetic in at most $\lceil n/s \rceil$ iterations, but the interesting case is when the method convergence in many fewer than $\lceil n/s \rceil$ iterations. In exact arithmetic, block CG reduces to CG when $s = 1$, i.e., CG is a particular case of block CG when only one right hand side of (1) is solved. Already in [13] it was suggested that block CG can be used to accelerate the convergence of CG for a single right hand side, i.e., for a system of the form $Ax = b$, and we have this situation very much in mind in our investigations.

From the CG theory, one can observe three phases of rate of convergence: sublinear, linear and superlinear [1, 2, 23, 24]. The characterization of each of the aforementioned phases and their respective transitions are essential since they strongly affect the rate of convergence of the iterative method. In this context, several papers analyze the transition phases for CG, in particular, the transition between linear and superlinear, as well as when the superlinear phase occurs [2, 20, 23, 24]. In the context of block CG, it is known that in certain circumstances the method exhibits superlinear behavior [18], but the conditions for this occurrence and the relation with the block size has not been well determined.

Superlinear behavior was studied in the framework of Krylov subspace methods by several authors [17, 19, 23, 25]. We can find in the literature two types of *a posteriori*

*This version dated 11 July 2021

Funding: Christian E. Schaerer: his research is partially supported by PRONII and by CONACYT-PY under project 14-INV186. Daniel B. Szyld: his research is supported in part by the U.S. National Science Foundation under grant DMS-1418882 and U.S. Department of Energy under grant DE-SC-0016578. Pedro Torres acknowledges the financial support of Scholarship-FEEI-CONACYT-PROCIENCIA.

†Polytechnic School, National University of Asuncion, San Lorenzo, Central, Paraguay. P.O.Box: 2111 SL. (cschaer@pol.una.py, pjtorres@pol.una.py). Corresponding author: P. J. Torres.

‡Department of Mathematics, Temple University (038-16), 1805 N. Broad Street, Philadelphia, PA 19122-6094, USA. (Email: szyld@temple.edu).

bounds for analyzing the superlinear convergence properties of CG. Namely, the work of van der Sluis and van der Vorst [23, 25] using spectral information (and Ritz values), and that of Simoncini and Szyld [17, 19] where angles between subspaces are considered. However, to the best of our knowledge, the superlinear behavior on block CG has not received enough attention and, in particular, the relationship with the block size s. In this paper, we use an *a posteriori* approach to gain some insight in what circumstances the superlinear behavior commences. We show that the bounds capture the superlinearity, and in particular the new bound captures well the slope of the block residual superlinear behavior. In addition, the numerical results illustrate that block CG captures clusters of eigenvalues (or repeated eigenvalues) thus accelerating the convergence of the method. In these experiments, it can be observed that the larger the blocks the faster the convergence, as one would intuitively expect, but in addition, one can see that larger block sizes induce an earlier onset of the superlinear phase.

Throughout this paper, calligraphic letters $\mathcal{A}$, $\mathcal{H}$ and $\mathcal{Z}$ denote square $s \times s$ matrices and upper case letters A, V, D and H denote square $n \times n$ matrices and $\mathbf{R}$, $\mathbf{X}$, $\mathbf{U}$, $\mathbf{W}$ and $\mathbf{B}$ denote rectangular $n \times s$ matrices, matrix polynomials are denoted with upper case Greek letters (e.g., Φ, Ω, Ξ). Scalars are denoted with lower case Greek letters (e.g., λ, γ, α) and integers are normally denoted as i, j, k, m and n. A subscript on a matrix, vector, or scalar denotes an iteration number. For simplicity, we consider only real matrices, although the generalization to complex matrices is direct.

This article is organized as follows. In §2 we present background material for the block-polynomial formulation of block CG and for the matrix polynomial theory (developed in [12] for block Krylov subspace methods). In §3, the *a posteriori* models are introduced. The first uses invariant subspaces (see §3.1) to explain the phenomenon and it is a particular case of the model introduced in [17]. In §3.2, using the block CG formulation and the block matrix polynomial theory approach, we propose an extension of the *a posteriori* bound introduced in [23] to analyze the superlinear convergence behavior of the block conjugate gradient. Numerical examples and comparison of the bounds are presented at §4.

2. Block-Polynomial Formulation of block CG. In this section we review some concepts related to block CG, its formulation as a minimization problem and the block formulation using a matrix-polynomial approach. In addition, we present some relationships between the formulations that we use in the next sections.

At each step m, block CG searches for the approximate solution on a specific subspace denoted by $\mathbb{K}_m(A, \mathbf{R}_0)$ known as the block Krylov subspace [7, 15]. There are several possible definitions for the subspace $\mathbb{K}_m(A, \mathbf{R}_0)$. In this article, we consider the classical definition [3, 4, 5, 8, 9]; i.e., let $\mathbf{X}_0$ be an arbitrary initial approximation to the solution of the system (1) and $\mathbf{R}_0 := \mathbf{B} - A\mathbf{X}_0$ its associated initial residual; let $\mathbb{S} \subseteq \mathbb{R}^{s\times s}$ be a vector subspace containing the identity $\mathcal{I}_s$ and closed under matrix multiplication and conjugate transposition, then the mth block Krylov subspace (corresponding to A, $\mathbf{R}_0$ of system (1), and $\mathbb{S}$) is defined as $\mathbb{K}_m^{\mathbb{S}}(A, \mathbf{R}_0) := \operatorname{span}^{\mathbb{S}}\{\mathbf{R}_0, A\mathbf{R}_0, \ldots, A^{m-1}\mathbf{R}_0\}$, in practical terms, this is equivalent to the following definition considered in this paper

$$\mathbb{K}_m(A, \mathbf{R}_0) := \left\{ \sum_{k=0}^{m-1} A^k \mathbf{R}_0 \mathcal{C}_k : \mathcal{C}_k \in \mathbb{S} \right\}, \tag{2}$$

where for simplicity we drop the superscript $\mathbb{S}$.

To express block CG as a minimization problem we define an appropriate inner-product. To this end, for any two real $n \times s$ block vectors $\mathbf{V}$ and $\mathbf{W}$, and a s.p.d. $n \times n$ matrix Z, we define the following inner product, named matrix Z-Frobenius inner product [4],

$$\langle \mathbf{V}, \mathbf{W} \rangle_{Z\text{-}F} := \operatorname{tr}(\mathbf{V}^* Z \mathbf{W}) = \sum_{i=1}^{s} \langle v_i, w_i \rangle_Z \,, \tag{3}$$

where $\mathbf{V} = [v_1, \ldots, v_s]$ and $\mathbf{W} = [w_1, \ldots, w_s]$.

Using the norm $\|\cdot\|$ induced by the inner product (3) with $Z = A^{-1}$, one can write the approximate mth step minimization A^{-1}-F norm of the residual $\mathbf{R}_m$ as

$$\|\mathbf{R}_m\|^2_{A^{-1}\text{-}F} = \min_{\mathbf{D} \in A\mathbb{K}_m} \|\mathbf{R}_0 - \mathbf{D}\|^2_{A^{-1}\text{-}F}. \tag{4}$$

The solution of the minimization problem (4) is denoted by $\mathbf{D}^\star$.

2.1. Block Lanczos Formulation. Let $\mathbf{R}_0 = \mathbf{U}_0 \mathcal{B}_0$ be the QR-factorization of $\mathbf{R}_0$, where $\mathbf{U}_0$ and $\mathcal{B}_0$ are real $n \times s$ and $s \times s$ matrices, respectively. The block Lanczos algorithm for a symmetric matrix A generates a sequence $\{\mathbf{U}_i\}$ for $i = 0, 1, 2 \ldots, m$, by the three-term recurrence

$$\mathbf{U}_{i+1}\mathcal{B}_{i+1} = \mathbf{M}_i = A\mathbf{U}_i - \mathbf{U}_i\mathcal{A}_i - \mathbf{U}_{i-1}\mathcal{B}_i^T, \tag{5}$$

where $\mathbf{U}_{-1} = \mathbf{0}$, $\mathcal{A}_i = \mathbf{U}_i^* A \mathbf{U}_i$ and $\mathbf{U}_{i+1}\mathcal{B}_{i+1}$ is the QR-factorization of $\mathbf{M}_i$ with $\mathbf{U}_{i+1}$ orthogonal and $\mathcal{B}_{i+1}$ upper triangular; see, e.g, [6]. At each iteration step m, the following matrix equation holds

$$A[\mathbf{U}_0, \mathbf{U}_1, \ldots, \mathbf{U}_{m-1}] = [\mathbf{U}_0, \mathbf{U}_1, \ldots, \mathbf{U}_{m-1}]T_m + \mathbf{U}_m \mathcal{B}_m E_m \tag{6}$$

where $E_m = [0_s, 0_s, \ldots, \mathcal{I}_s] \in \mathbb{R}^{s \times sm}$ and T_m is the following block tridiagonal matrix of dimension $ms \times ms$

$$T_m = \begin{pmatrix} \mathcal{A}_0 & \mathcal{B}_1^T & & & \\ \mathcal{B}_1 & \mathcal{A}_1 & \ddots & & \\ & \mathcal{B}_2 & \ddots & & \\ & & \ddots & \mathcal{A}_{m-2} & \mathcal{B}_{m-1}^T \\ & & & \mathcal{B}_{m-1} & \mathcal{A}_{m-1} \end{pmatrix}. \tag{7}$$

Matrix T_m is the orthogonal projection and restriction of matrix A onto the block Krylov subspace $\mathbb{K}_m(A, \mathbf{R}_0)$, and its eigenvalues approximate the eigenvalues of A [6]. The Lanczos iteration constructs an orthonormal basis $W_m = [\mathbf{U}_0, \mathbf{U}_1, \ldots, \mathbf{U}_{m-1}]$ for the block Krylov subspace $\mathbb{K}_m(A, \mathbf{R}_0)$. The expression (6) can be rewritten as

$$A\, W_m = W_{m+1}\, \tilde{T}_m. \tag{8}$$

where $T_m := [I_{ms}, 0]\, \tilde{T}_m$ is a real block tridiagonal matrix of dimension $(m+1)s \times ms$.

The approximate solution of the linear systems produced by block CG at the mth iteration is given by

$$\mathbf{X}_m = \mathbf{X}_0 + W_m Y_m, \tag{9}$$

where $Y_m = [y_1^T, \ldots, y_m^T]^T$ with $y_i \in \mathbb{R}^{s\times s}$ is obtained by solving the equation

$$T_m Y_m = \mathcal{B}_0 E_1^* \tag{10}$$

with $E_1 = [I_s, 0_s, \ldots, 0_s] \in \mathbb{R}^{s\times sm}$. Since $\mathbf{R}_0 = \mathbf{U}_0\mathcal{B}_0$, then equation (10) is equivalent to $W_m T_m Y_m = \mathbf{R}_0$. In addition, at each block iteration it is possible to compute the residual of the solution without explicitly computing the solution, using the expression $\mathbf{R}_m = -\mathbf{U}_m\mathcal{B}_m E_m Y_m$ which is obtained as follows (see, e.g., [4], [15]):

$$\begin{aligned}
\mathbf{R}_m &= \mathbf{B} - A\mathbf{X}_m && \text{by definition of } \mathbf{R}_m\\
&= \mathbf{B} - A(\mathbf{X}_0 + W_m Y_m) && \text{by expression (9)}\\
&= \mathbf{R}_0 - AW_m Y_m && \text{by definition of } \mathbf{R}_0\\
&= \mathbf{R}_0 - W_m T_m Y_m - \mathbf{U}_m\mathcal{B}_m E_m Y_m && \text{by identity (6)}\\
&= -\mathbf{U}_m\mathcal{B}_m E_m Y_m && \text{by identity (10).}
\end{aligned} \tag{11}$$

Notice that $\mathbf{R}_m = \mathbf{R}_0 - \mathbf{D}^\star$ and $\mathbf{D}^\star = AW_m Y_m$ in (4).

2.2. Block matrix polynomial formulation. We are interested in developing a block formulation using a matrix polynomial approach. To this end, some notation is introduced. Let $\mathbb{P}_{m,s}$ be the space of matrix-value polynomials with elements of the form

$$\Upsilon_m(\eta) = \sum_{i=0}^{m} \eta^i \mathcal{C}_i \tag{12}$$

where $\eta \in \mathbb{R}$ and $\mathcal{C}_i$ are real $s \times s$ matrices. In order to define matrix polynomials, we recall the operation introduced in [12],

$$\Upsilon_m(A) \circ \mathbf{X} = \sum_{i=0}^{m} A^i \mathbf{X} \mathcal{C}_i, \tag{13}$$

where A is any $n \times n$ matrix, $\mathbf{X}$ is a block $n \times s$ vector and '$\circ$' is the Graag operator.

Denote by $\mathbb{G}_{m,s} \subset \mathbb{P}_{m,s}$ the subspace of matrix-value polynomials with elements of the form $\Upsilon_m(\eta) = \mathcal{I}_s - \sum_{i=0}^{m-1} \eta^{i+1}\mathcal{C}_i$. Hence, using the nomenclature (13) and the subspace $\mathbb{G}_{m,s}$, the residual $\mathbf{R}_m$ of block CG at the mth iteration can be expressed in terms of matrix polynomials as

$$\mathbf{R}_m = \Psi_m(A) \circ \mathbf{R}_0 = \mathbf{R}_0 - \sum_{i=0}^{m-1} A^{i+1}\mathbf{R}_0\mathcal{G}_i, \tag{14}$$

where $\Psi_m \in \mathbb{G}_{m,s}$, and $\mathcal{G}_i$ with $i = 1, \ldots, m-1$ are $s \times s$ matrices. Hence, the block CG iteration (4) using matrix-value polynomial with A and $\mathbf{R}_0$ as arguments can be expressed as follows

$$\|\mathbf{R}_m\|_{A^{-1}\text{-}F} = \min_{\Psi_m \in \mathbb{G}_{m,s}} \|\Psi_m(A) \circ \mathbf{R}_0\|_{A^{-1}\text{-}F} = \|\Phi_m(A) \circ \mathbf{R}_0\|_{A^{-1}\text{-}F} \tag{15}$$

where $\Phi_m(\eta) \in \mathbb{G}_{m,s}$ is the solution of the minimization problem.

The three-term recurrence (6) of the Block Lanczos algorithm for a symmetric matrix A can be written in matrix polynomial form as follows [16]. Each matrix $\mathbf{U}_i$ in the recurrence in (6) can be written as a linear combinations of matrices

$A^i\mathbf{R}_0 \in \mathbb{K}_m(A,\mathbf{R}_0)$ for $i = 0, 1, \ldots, m$. Therefore we can set $\mathbf{U}_i = \Gamma_i(A) \circ \mathbf{U}_0$, and consequently, (6) can be rewritten in matrix polynomial form as follows [12]:

$$\eta P_{m-1}(\eta) = P_{m-1}(\eta)T_m + \Gamma_m(\eta)\mathcal{B}_m E_m, \tag{16}$$

where $P_{m-1}(\eta) := [\Gamma_0(\eta), \Gamma_1(\eta), \ldots, \Gamma_{m-1}(\eta)]$ with $\Gamma_i \in \mathbb{P}_{i,s}$.

It can be observed from (16) that $\det(\lambda I - T_m) = 0$ if and only if $\det(\Gamma_m(\lambda)) = 0$. Therefore, the eigenvalues of T_m are the latent roots of $\Gamma_m(\lambda)$, hence coinciding with the Ritz values of A associated with $\mathbb{K}_m(A,\mathbf{R}_0)$. In addition, the matrix polynomials $\Gamma_m(\lambda)$ and $\Phi_m(\lambda)$ represent the block CG process dynamics but from different perspective [4, 16]. In the following proposition we show that the latent roots of these matrix polynomials are the same.

Proposition 1. The latent roots of the block CG polynomial $\Phi_m(\eta)$ coincide with the latent roots of $\Gamma_m(\eta)$. Hence they are also the eigenvalues of T_m and the Ritz values of the matrix A associated with $\mathbb{K}_m(A,\mathbf{R}_0)$.

Proof. From expression (11) and using matrix value representation, the block residual can be expressed as follows,

$$\mathbf{R}_m = -(\Gamma_m(A) \circ \mathbf{U}_0)\mathcal{B}_m E_m Y_m.$$

Using equation (14) we can arrive to the following equality in matrix polynomial form

$$\Phi_m(\eta) = -\Gamma_m(\eta)\mathcal{B}_m E_m Y_m,$$

then the latents roots of $\Phi_m(\eta)$ and $\Gamma_m(\eta)$ are the same. ∎

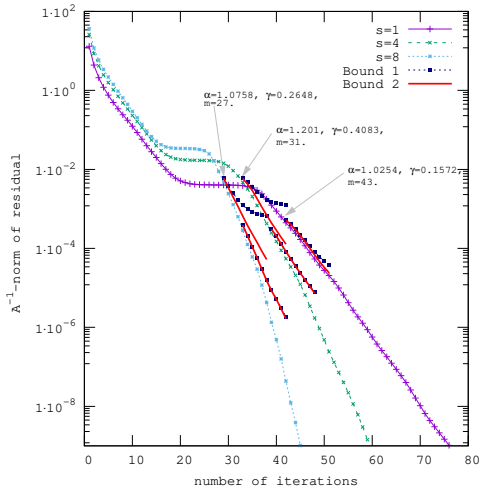

Fig. 1: Example 4.3. Residual convergence behavior for the block CG $\|\mathbf{R}_{m+j}\|_{A^{-1}\text{-}F}$ for $s = 1, 4, 8$, bounds $b_{1,j}$ and $b_{2,j}$ correspond to expressions (37). Parameters $k_1 = 1$ and $k_2 = 0$.

3. The *a posteriori* models for block CG. As mentioned in the introduction, block CG can present phases in its convergence. Figure 1 shows an example of the residual norm behavior for several block sizes (computational details about this

example are presented in §4.3). In this example, one can observe the phases of convergence of block CG. After a convergence plateau, the superlinear convergence arises. We also present in Figure 1 the *a posteriori* bounds discussed in this article. Note in particular that Bound 2 which is introduced in §3.2 captures well the behavior of the block CG residual.

In the context of the *a posteriori* bounds discussed in this paper two issues are to be addressed: 1) how well the bounds for block CG capture the behavior of the superlinear convergence rate in terms of the Ritz values and its convergence to their corresponding eigenvalues, and 2) the insight that the bounds can provide on the superlinear behavior in terms of how the block size affects the onset of the superlinear convergence.

In this section, two *a posteriori* bounds that consider the superlinear convergence are analyzed. Both bounds compare the convergence behavior of a block CG process beginning at a certain step m, with another residual reduction process, called a comparison process; see expression (17) below. The first bound is a particular case of the results presented in [17], the bound is computed using invariant subspaces and Ritz vectors, and we call it a *subspace-based bound*. For the second bound we introduce an extension of the approach introduced in [24]. This bound is computed using spectral information and the Ritz values, and we call it a *spectrum-based bound*.

Let $\lambda_1, \ldots, \lambda_n$ and $v_1, \ldots, v_n$ be the eigenvalues and eigenvectors associated with the matrix A, chosen such that they form an orthonormal basis. Then $A = V\Lambda V^T$ is a spectral decomposition of matrix A with $V = [v_1, \ldots, v_n]$ and $\Lambda = \operatorname{diag}[\lambda_1, \ldots, \lambda_n]$. The comparison process is a residual sequence, in which the components on the chosen invariant subspace have been eliminated. To define this more precisely let Π_Q be a spectral projector onto a simple invariant subspace $\mathbb{R}(Q)$[1] of the matrix A with dimension k, where Q is an $n \times k$ matrix whose columns are k eigenvectors of A. Recall that a simple invariant subspace is such that its orthogonal complement is also an invariant subspace. The spectral projector is constructed as $\Pi_Q = QQ^T$ and in this case it is also an orthogonal projector with respect to the A^{-1}-F inner product $\langle \cdot, \cdot \rangle_{A^{-1}\text{-}F}$ since the matrix A^{-1} commutes with its spectral projector, i.e., $\Pi_Q A^{-1} = A^{-1}\Pi_Q$.

The block comparison process is defined as

$$\|\bar{\mathbf{R}}_j\|_{A^{-1}\text{-}F} = \min_{\mathbf{D} \in A\mathbb{K}_j(A, \bar{\mathbf{R}}_0)} \|\bar{\mathbf{R}}_0 - \mathbf{D}\|_{A^{-1}\text{-}F}, \qquad \bar{\mathbf{R}}_0 = (I - \Pi_Q)\mathbf{R}_m, \tag{17}$$

where $\bar{\mathbf{R}}_j$ is the residual to the jth step of the CG process started with a modified initial vector $\mathbf{R}_m$, where all components in the invariant subspace $\mathbb{R}(Q)$ have been eliminated.

The bounds that are going to be presented in this section depend on the choice of either a certain subspace $\mathbb{Y}$ (to be defined latter) or in the approximation of certain number of eigenvalues of the matrix A. It was observed in [13] that the convergence of CG depends on how quickly the extreme eigenvalues are approximated by the Ritz values. As a consequence, we concentrate our efforts in capturing the extreme parts of the spectrum.

3.1. Subspace-based bound for block CG. Here the focus consists in establishing an upper bound for the block CG defined by expression (4). The computation of the bound assumes that the approximate solution at the $m-$th step $\mathbf{X}_m$ is known,

[1] Here and elsewhere in the paper $\mathbb{R}(Q)$ denotes the range of the matrix Q.

and consequently, the corresponding residual $\mathbf{R}_m$. The next theorem is based on a general framework presented in [17] to compute an upper bound for the norm of $\mathbf{R}_{m+j}$.

THEOREM 1 (Subspace-based bounds for block Conjugate Gradient [17]). *Consider an $m \times k$ real matrix Y, whose columns are a basis of a k-dimensional subspace of $A\mathbb{K}_m(A, R_0)$. Let Π_Y be the A^{-1}-orthogonal projector onto $\mathbb{R}(Y)$, and let $\gamma = \|(I - \Pi_Y)\Pi_Q\|_{A^{-1}\text{-}F}$. Then*

$$\|\mathbf{R}_{m+j}\|_{A^{-1}\text{-}F} \leq \min_{\mathbf{D}\in A\mathbb{K}_j(A,\mathbf{R}_m)} \Big\{ \|(I-\Pi_Q)(\mathbf{R}_m - \mathbf{D})\|_{A^{-1}\text{-}F} + \gamma_m \|\Pi_Q(\mathbf{R}_m - \mathbf{D})\|_{A^{-1}\text{-}F} \Big\} \tag{18}$$

$$\leq \sqrt{2} \min_{\mathbf{D}\in A\mathbb{K}_j(A,\mathbf{R}_m)} \left\| \begin{bmatrix} (I-\Pi_Q) \\ \gamma\Pi_Q \end{bmatrix} (\mathbf{R}_m - \mathbf{D}) \right\|_\star, \tag{19}$$

where $\|\cdot\|_\star$ is an induced vector norm from the following inner product. Let $u_i, v_i \in \mathbb{R}^n$, $i = 1, 2$; then, if $u^T = \begin{bmatrix} u_1^T, u_2^T \end{bmatrix}$, $v^T = \begin{bmatrix} v_1^T, v_2^T \end{bmatrix}$, $\langle u, v\rangle_\star = \langle u_1, v_1\rangle_{A^{-1}} + \langle u_2, v_2\rangle_{A^{-1}}$.

The computation of the upper bound is possible using the expression (19), which is a reformulation of (18) as a least squares problem of dimension $2n$. The least-squares problem (19) is well posed as long as $\mathbb{R}(Q) \cap A\mathbb{K}_j(A, \mathbf{R}_m) = \{0\}$. To describe the terms in expression (18), consider $\mathbf{D}_\star$ to be the least squares solution of expression (19) and replacing it in expression (18), then two terms are obtained: α_1 and α_2. The term $\alpha_1 := \|(I - \Pi_Q)(\mathbf{R}_m - \mathbf{D}_\star)\|_{A^{-1}\text{-}F}$ measures the contribution to the bound of the null space of the projector Π_Q. In the context of block CG, it makes sense to consider an orthogonal projector, since the invariant subspace of the symmetric positive definite matrix A can be decomposed into orthogonal subspaces.

The term $\alpha_2 := \gamma\|\Pi_Q(\mathbf{R}_m - \mathbf{D}_\star)\|_{A^{-1}\text{-}F}$ measures the contribution to the bound of the projection Π_Q weighted by the factor γ. In this way, if it is computing the bound at a certain step where the residual components on the eigenvectors (which are in $\mathbb{R}(Q)$) have not been eliminated yet, then the term α_2 would have a considerable effect on the bound. However, if the residual component on the eigenvectors has been eliminated (or almost eliminated), the contribution of the term α_2 would be negligible to the bound. The latter means that the subspaces $\mathbb{R}(Q)$ and $\mathbb{R}(Y)$ are very close ($\gamma \ll 1$) and $\|\Pi_Q(\mathbf{R}_m - \mathbf{D}_\star)\|_{A^{-1}\text{-}F} \approx 0$. In this case, the more relevant term is α_1.

The terms α_1 and α_2 compensate one another, since $\mathbb{R}(Q) \bigoplus \mathbb{R}(Q)^\perp = \mathbb{R}^n$, therefore they introduce in the analysis information of the whole space. In this article, for simplicity the case of $\dim \mathbb{R}(Y) = \dim \mathbb{R}(Q) = k$ is considered. In this case, the value of γ is such that

$$\gamma = \|(I - \Pi_Y)\Pi_Q\|_{A^{-1}\text{-}F} = \|\Pi_Y - \Pi_Q\|_{A^{-1}\text{-}F} = \sin\varphi \leq 1, \tag{20}$$

where φ is the maximum canonical angle between $\mathbb{R}(Y)$ and $\mathbb{R}(Q)$; see, e.g., [11, p. 56] and [21, p. 92] for details. Consequently, in block CG, γ is exactly the opening or gap between the subspaces $\mathbb{R}(Y)$ and $\mathbb{R}(Q)$; see, e.g., [6, 21]. It is important to remark that this result is more restrictive than the general definition of γ considered in [17], where it can have values larger than 1.

For the numerical experiments (Section 4), the matrix Y is constructed with columns of the form $y_i = Az_i$, $z_i \in \mathbb{K}_m(A, \mathbf{R}_0)$, and z_i are taken to be Ritz vectors. As a consequence, there is a dependence of γ on the iteration m, hence instead of using γ, we denote this dependence by writing γ_m.

3.2. Spectral-based bound for block CG. In this section, we present a superlinear model based on the spectral information for the block CG algorithm. This is done by using the background material provided in [12]. Inspired by the development of the theory in [24], key steps consist in using the optimality property of block CG (expression (4)) and constructing an artificial process using an auxiliar matrix polynomial; taking into account that the Ritz values coincide with the latent roots of $\Phi_m(\lambda)$ and converge to the eigenvalues of matrix A for a sufficiently large m [16].

For our analysis, the following result (introduced in [12]) is useful.

LEMMA 2. [12] *Let $\Upsilon_l(\eta) = \sum_{i=0}^{l} \eta^i \mathcal{C}_i$ be any matrix polynomial where $\mathcal{C}_i$ are $s \times s$ matrices, and let A be a $n \times n$ matrix, $\mathbf{Z}$ a $n \times s$ matrix and S any invertible matrix of order n. Then the following result holds,*

$$\Upsilon_l(A) \circ \mathbf{Z} = S\Upsilon_l(S^{-1}AS) \circ (S^{-1}\mathbf{Z}). \tag{21}$$

Using Lemma 2, the expression (15) is rewritten as a weighted sum with the eigenvalues as arguments. The procedure introduced in the following lemma (adapted from one presented in [12, Ch. 4, expression (4.7)]) is important to understand the next theorems.

LEMMA 3. *Let $[w_1, w_2, \ldots, w_n]^T = V^T R_0$ be the components of the block initial residual on the eigenbasis, where w_i's ($i = 1, \ldots, n$) are $s \times 1$ matrices. Consider a spectral decomposition of $A = V\Lambda V^T$ and $\mathbf{R}_m = \Phi_m(A) \circ \mathbf{R}_0$ the residual of block CG at iteration m. Then,*

$$\|\mathbf{R}_m\|^2_{A^{-1}\text{-}F} = \operatorname{tr}\left(\mathbf{R}_m^T A^{-1} \mathbf{R}_m\right) = \operatorname{tr}\left[\sum_{i=1}^{n} \frac{1}{\lambda_i} \Phi_m^T(\lambda_i) w_i w_i^T \Phi_m(\lambda_i)\right]. \tag{22}$$

Proof. Using Lemma 2 and noting that $VV^T = I_n$ we can write

$$\begin{aligned}\mathbf{R}_m &= \Phi_m(A) \circ \mathbf{R}_0 \\ &= V\Phi_m(V^TAV) \circ V^T\mathbf{R}_0 = V\Phi_m(\Lambda) \circ \begin{bmatrix} w_1^T \\ w_2^T \\ \vdots \\ w_n^T \end{bmatrix} = V \begin{bmatrix} w_1^T\Phi_m(\lambda_1) \\ w_2^T\Phi_m(\lambda_2) \\ \vdots \\ w_n^T\Phi_m(\lambda_n) \end{bmatrix}.\end{aligned}$$

The results follows taking the norm $\|\cdot\|_{A^{-1}\text{-}F}$. ∎

Lemma 3 shows that the block residual can be expressed as the trace of a sum of $s \times s$ matrices with the matrix polynomial decoupled on each eigenvalue, and the weights $w_i w_i^T$ with $i = 1, \ldots, n$ are $s \times s$ matrices of rank-one, and symmetric, positive semi-definitive. Note that for $s = 1$, Lemma 3 reduces to the CG case. The decoupling of the eigenvalues and the elimination of the operator '$\circ$' simplify the development of a superlinear bound in the block case.

For the sake of simplicity, we state the following theorem for the superlinear bound to the case of $k_1 = 1$ and $k_2 = 0$. That is, we consider the eigenpairs corresponding to the lowest part of the spectrum (λ_1, v_1) and its corresponding lowest Ritz value at the iteration m denoted $\theta_1^{(m)}$.

THEOREM 4. *Let $\mathbf{R}_{m+j}$ be the block CG residual at the $(m+j)$th iteration and $\bar{\mathbf{R}}_j$ be the residual after j iterations of block CG applied to $\bar{\mathbf{R}}_0 = (I - \Pi_Q)\mathbf{R}_m$, with $\Pi_Q = v_1 v_1^T$ and $\mathbf{R}_m = \Phi_m(A) \circ \mathbf{R}_0$, i.e.,*

$$\bar{\mathbf{R}}_j = \Psi_j(A) \circ \bar{\mathbf{R}}_0, \tag{23}$$

where $\Psi_j(\lambda) \in \mathbb{G}_{m,s}$ is the corresponding matrix polynomial of degree j for the new block CG residual. Then,

$$\|\mathbf{R}_{m+j}\|_{A^{-1}\text{-}F} \leq \alpha_{m,1,0}\|\bar{\mathbf{R}}_j\|_{A^{-1}\text{-}F}, \tag{24}$$

where $\alpha_{m,1,0} = \left[\frac{\theta_1^{(m)}}{\lambda_1}\max_{\lambda_i\neq\lambda_1}\frac{|\lambda_i-\lambda_1|}{|\lambda_i-\theta_1^{(m)}|}\right]$

Proof. Let $\Omega_m(\eta)$ be a matrix-value polynomial constructed as follows,

$$\Omega_m(\eta) = \frac{\theta_1^{(m)}}{\lambda_1}(\eta-\lambda_1)(\eta-\theta_1^{(m)})^{-1}\Phi_m(\eta), \tag{25}$$

and since $\Omega_m(0) = \mathcal{I}_s$, $\Omega_m(\eta) \in \mathbb{G}_{m,s}$. By the optimality property of block CG (15) we have the following relation,

$$\|\mathbf{R}_{m+j}\|_{A^{-1}\text{-}F} \leq \|\Psi_j(A)\circ[\Omega_m(A)\circ\mathbf{R}_0]\|_{A^{-1}\text{-}F}\,.$$

Following a similar procedure used in Lemma 3, we have

$$\|\mathbf{R}_{m+j}\|^2_{A^{-1}\text{-}F} \leq \left\| V\begin{bmatrix} w_1^T\Omega_m(\lambda_1)\Psi_j(\lambda_1)\\ w_2^T\Omega_m(\lambda_2)\Psi_j(\lambda_2)\\ \vdots\\ w_n^T\Omega_m(\lambda_n)\Psi_j(\lambda_n)\end{bmatrix}\right\|^2_{A^{-1}\text{-}F}. \tag{26}$$

Using expression (25), the right hand side of inequality (26) can be written as

$$\begin{aligned}\left\| V\begin{bmatrix} w_1^T\Omega_m(\lambda_1)\Psi_j(\lambda_1)\\ w_2^T\Omega_m(\lambda_2)\Psi_j(\lambda_2)\\ \vdots\\ w_n^T\Omega_m(\lambda_n)\Psi_j(\lambda_n)\end{bmatrix}\right\|^2_{A^{-1}\text{-}F} &\\ = \left\| V\begin{bmatrix} w_1^T\frac{\theta_1^{(m)}}{\lambda_1}(\lambda_1-\lambda_1)(\lambda_1-\theta_1^{(m)})^{-1}\Phi_m(\lambda_1)\Psi_j(\lambda_1)\\ w_2^T\frac{\theta_1^{(m)}}{\lambda_1}(\lambda_2-\lambda_1)(\lambda_2-\theta_1^{(m)})^{-1}\Phi_m(\lambda_2)\Psi_j(\lambda_2)\\ \vdots\\ w_n^T\frac{\theta_1^{(m)}}{\lambda_1}(\lambda_n-\lambda_1)(\lambda_n-\theta_1^{(m)})^{-1}\Phi_m(\lambda_n)\Psi_j(\lambda_n)\end{bmatrix}\right\|^2_{A^{-1}\text{-}F}&.\end{aligned} \tag{27}$$

Since by construction the first row on the right hand side of (26) (equivalently expression (27)) is zero, then evaluating the matrix polynomial $\Omega(\lambda)$ on each eigenvalue and taking into account that the matrices $w_iw_i^T$ are positive semi-definitive, the

following is obtained

$$
\begin{aligned}
(28)\quad & \left\| V \begin{bmatrix} w_1^T \frac{\theta_1^{(m)}}{\lambda_1}(\lambda_1-\lambda_1)(\lambda_1-\theta_1^{(m)})^{-1}\Phi_m(\lambda_1)\Psi_j(\lambda_1) \\ w_2^T \frac{\theta_1^{(m)}}{\lambda_1}(\lambda_2-\lambda_1)(\lambda_2-\theta_1^{(m)})^{-1}\Phi_m(\lambda_2)\Psi_j(\lambda_2) \\ \vdots \\ w_n^T \frac{\theta_1^{(m)}}{\lambda_1}(\lambda_n-\lambda_1)(\lambda_n-\theta_1^{(m)})^{-1}\Phi_m(\lambda_n)\Psi_j(\lambda_n) \end{bmatrix} \right\|^2_{A^{-1}\text{-}F} \\
&= \left\| V \begin{bmatrix} 0 \\ w_2^T \frac{\theta_1^{(m)}}{\lambda_1}(\lambda_2-\lambda_1)(\lambda_2-\theta_1^{(m)})^{-1}\Phi_m(\lambda_2)\Psi_j(\lambda_2) \\ \vdots \\ w_n^T \frac{\theta_1^{(m)}}{\lambda_1}(\lambda_n-\lambda_1)(\lambda_n-\theta_1^{(m)})^{-1}\Phi_m(\lambda_n)\Psi_j(\lambda_n) \end{bmatrix} \right\|^2_{A^{-1}\text{-}F} \\
&= \left\| V \begin{bmatrix} 0 \\ \frac{\theta_1^{(m)}}{\lambda_1}(\lambda_2-\lambda_1)(\lambda_2-\theta_1^{(m)})^{-1} w_2^T\Phi_m(\lambda_2)\Psi_j(\lambda_2) \\ \vdots \\ \frac{\theta_1^{(m)}}{\lambda_1}(\lambda_n-\lambda_1)(\lambda_n-\theta_1^{(m)})^{-1} w_n^T\Phi_m(\lambda_n)\Psi_j(\lambda_n) \end{bmatrix} \right\|^2_{A^{-1}\text{-}F} \\
&= \frac{\theta_1^{(m)}}{\lambda_1} \operatorname{tr}\left[\sum_{i=2}^{n} (\lambda_i-\lambda_1)(\lambda_i-\theta_1^{(m)})^{-1} \frac{1}{\lambda_i} (\Phi_m(\lambda_i)\Psi_j(\lambda_i))^T w_i w_i^T \Phi_m(\lambda_i)\Psi_j(\lambda_i) \right].
\end{aligned}
$$

In the last expression we take the maximum over the scalar factors,

$$
\leq \left[\frac{\theta_1^{(m)}}{\lambda_1} \max_{\lambda_i \neq \lambda_1} \frac{|\lambda_i-\lambda_1|}{|\lambda_i-\theta_1^{(m)}|} \right]^2 \operatorname{tr}\left[\sum_{i=2}^{n} \frac{1}{\lambda_i} (\Phi_m(\lambda_i)\Psi_j(\lambda_i))^T w_i w_i^T \Phi_m(\lambda_i)\Psi_j(\lambda_i) \right].
$$

Using Lemma 3 and since in the sum starts with $i = 2$, we obtain the following expression to the block CG residual $\|\mathbf{R}_{m+j}\|^2_{A^{-1}\text{-}F}$

$$
\begin{aligned}
\|\mathbf{R}_{m+j}\|^2_{A^{-1}\text{-}F} &\leq \left[\frac{\theta_1^{(m)}}{\lambda_1} \max_{\lambda_i \neq \lambda_1} \frac{|\lambda_i-\lambda_1|}{|\lambda_i-\theta_1^{(m)}|} \right]^2 \|\Psi_j(A) \circ \Phi_m(A) \circ (I-\Pi_Q)\mathbf{R}_0\|^2_{A^{-1}\text{-}F} \\
&= \left[\frac{\theta_1^{(m)}}{\lambda_1} \max_{\lambda_i \neq \lambda_1} \frac{|\lambda_i-\lambda_1|}{|\lambda_i-\theta_1^{(m)}|} \right]^2 \left\|\bar{\mathbf{R}}_j\right\|^2_{A^{-1}\text{-}F}. \qquad (29)
\end{aligned}
$$

The result follows taking the square root. ∎

It is important to remark that the behavior of the auxiliary matrix polynomial $\Omega_m(\lambda)$ is such that the effect of the lowest Ritz value is removed, and when the Ritz value $\theta_1^{(m)}$ converges to λ_1 the polynomial behaves almost as $\Phi_m(\lambda)$, since

$$
\mathcal{I}_s \approx (\eta-\lambda_1)(\eta-\theta_1^{(m)})^{-1}.
$$

For a generalization, we follow a similar line of reasoning for other parts of the spectrum. This yields the Theorem 5 which is a general version of Theorem 4 in the block CG context. Its proof follows by choosing a suitable set of eigenvalues to construct the auxiliary matrix polynomial $\Omega_m(\lambda)$.

In the followings theorem k_1 denotes the number of eigenvalues considered in the lowest part and k_2 the number of eigenvalues considered in the upper part of the spectrum.

THEOREM 5. *Let $\mathbf{R}_{m+j}$ be the block CG residual at the $m+j$th step and $\bar{\mathbf{R}}_j$ be the residual after j steps of block CG applied to $\bar{\mathbf{R}}_0 = (I - \Pi_Q)\mathbf{R}_m$, with $\Pi_Q = QQ^*$ and $\mathbf{R}_m = \Phi_m(A) \circ \mathbf{R}_0$, where $Q \in \mathbb{R}^{n\times k}$ with $k = k_1 + k_2$, and*

$$\bar{\mathbf{R}}_j = \Psi_j(A) \circ \bar{\mathbf{R}}_0, \tag{30}$$

where $\Psi_j(\lambda) \in \mathbb{P}_{m,s}$ is the corresponding block CG matrix polynomial of degree j. Then,

$$\|\mathbf{R}_{m+j}\|_{A^{-1}\text{-}F} \leq \alpha_{m,k_1,k_2} \left\|\bar{\mathbf{R}}_j\right\|_{A^{-1}\text{-}F}, \tag{31}$$

where α_{m,k_1,k_2} is given by

$$\alpha_{m,k_1,k_2} = \max_{j_1>k_1,\, j_2\geq k_2} \prod_{j=1}^{k_1} \frac{\theta_j^{(m)}}{\lambda_j} \left|\frac{\lambda_{j_1} - \lambda_j}{\lambda_{j_1} - \theta_j^{(i)}}\right| \prod_{j=1}^{k_2} \frac{\theta_{n+1-j}^{(m)}}{\lambda_{n+1-j}} \left|\frac{\lambda_{n+1-j} - \lambda_{n-j_2}}{\theta_{m+1-j}^{(m)} - \lambda_{n-j_2}}\right|. \tag{32}$$

Proof. Let $\Omega_m(\lambda)$ be a matrix polynomial constructed as follows,

$$\Omega_m(\lambda) = \prod_{j=1}^{k_1} \frac{\theta_j^{(m)}}{\lambda_j}(\lambda_{j_1} - \lambda_j)(\lambda_{j_1} - \theta_j^{(m)})^{-1} \times \prod_{j=1}^{k_2} \frac{\theta_{n+1-j}^{(m)}}{\lambda_{n+1-j}}(\lambda_{n+1-j} - \lambda_{n-j_2})(\theta_{m+1-j}^{(m)} - \lambda_{n-j_2})^{-1}\Phi_m(\lambda).$$

for $j_1 > k_1$ and $j_2 \geq k_2$, and since $\Omega_m(0) = \mathcal{I}_s$, $\Omega_m(\eta) \in \mathbb{G}_{m,s}$. The result follows using a similar procedure employed in Theorem 4. ∎

Theorem 5 shows that in this model the norm of block residual denoted by $\|\mathbf{R}_{m+j}\|_{A^{-1}\text{-}F}$ is bounded by an expression proportional to a comparison norm residual $\left\|\bar{\mathbf{R}}_j\right\|_{A^{-1}\text{-}F}$ and α_{m,k_1,k_2} is the proportional factor that controls the process. This factor is associated with the eigenvalues that are supposed to be deflated by the block CG up to the j-th iteration; see (32).

Remark 6. Consider the the matrix polynomial (25) and $s = 1$, then $\alpha_{m,1,0}$ (of expression (24)) takes the form

$$\alpha_{m,1,0} = \frac{\theta_1}{\lambda_1} \max_{\lambda_k\neq\lambda_1} \frac{\lambda_k - \lambda_1}{\lambda_k - \theta_1}, \tag{33}$$

i.e., it is the same bound obtained in [24] when studying superlinear bound in CG.

Remark 7. When there is an eigenvalue with algebraic multiplicity κ for instance in the lowest part of the spectrum, and $k_1 \leq \kappa$, and $k_2 = 0$, then the matrix polynomial $\Omega_m(\eta)$ takes the form

$$\Omega_m(\eta) = \prod_{j=1}^{k_1} \frac{\theta_j^{(m)}}{\lambda_j}(\lambda_{j_1} - \lambda_j)(\lambda_{j_1} - \theta_j^{(m)})^{-1}\Phi_m(\eta). \tag{34}$$

with $j_1 > k_1$, since $\Omega_m(0) = \mathcal{I}_s$, $\Omega_m(\eta) \in \mathbb{G}_{m,s}$. In this case $\alpha_{m,k_1,0}$ in Theorem 5 reduces to

$$\alpha_{m,k_1,0} = \max_{j_1>k_1} \prod_{j=1}^{k_1} \frac{\theta_j^{(m)}}{\lambda_j} \left|\frac{\lambda_{j_1} - \lambda_j}{\lambda_{j_1} - \theta_j^{(i)}}\right|. \tag{35}$$

4. Numerical Experiments. In this section, we present experimental examples supporting the theoretical observations introduced earlier in the paper. The order of the examples are as follows. Example 4.1 analyzes the behavior of the bounds for a single eigenvalue using a block size $s = 1$. With this choice of s the Block CG reduces to classical CG. This is done in order to compare our results with the results presented in [17, 24]. Example 4.2 analyzes the behavior of the bounds for capturing several eigenvalues simultaneously. Example 4.3 is designed to analyze the effect of the block size s on the convergence of block CG on a matrix with a single eigenvalue near the origin and smaller than the others. Example 4.4 is designed to study of the effect of the block size s in presence of a cluster of eigenvalues near the origin. In Example 4.5 the case of an eigenvalue with multiplicity κ in the lowest part of its spectrum is considered. In all these examples it suffices to consider appropriate diagonal matrices, whose diagonal entries represent the different eigenvalue distributions. Finally, in Example 4.6, we use a discrete 2D Poisson equation with an incomplete Cholesky factorization as a prototype of a matrix obtained of engineering or scientific common applications. In Table 1, we present a summary, as well as the values of k_1, k_2, and s used in the examples.

Table 1: Summary of experimental examples

		k_1	k_2	s
4.1	bounds for an isolated eigenvalue	1	0	1
4.2	bounds for several eigenvalues	4	0	1
4.3	varying s for an isolated eigenvalue	1	0	$1, 4, 8$
4.4	varying s for a cluster eigenvalues	6	0	$1, 2, 4, 8$
4.5	varying s for multiple eigenvalues	1	1	1
		2	0	1
		4	0	4
		5	0	4
4.6	preconditioned Poisson equation	1	0	1
		2	0	1
		4	0	4
		5	0	4

Example 4.1. In this example, a 100×100 diagonal matrix with eigenvalues 0.1, 0.2, 0.3, 0.4, 5, ... , 100 is considered. The right-hand side is a vector with all unit entries, the initial approximation $\mathbf{X}_0 = x_0$ is the null vector, and the initial residual is $\mathbf{R}_0 = b$; *i.e.*, the residual has equal components in all eigenvectors that form an eigenbasis so that no one eigendirection is favored. To compare the behavior of both bounds during the stages of convergence of the Ritz value θ_1 towards the smallest eigenvalue λ_1, Theorem 5 reduces to the superlinear bound presented in [24]. That is, we consider $k_1 = 1$, $k_2 = 0$ and $s = 1$. Following [25], three cases are studied, in the first two cases the Ritz values are in its final interval of convergence, i.e., $\lambda_1 \leq \theta_1^{(m)} < \lambda_2$ and the last case is outside of its final interval of convergence, i.e., $\lambda_2 < \theta_1^{(m)}$:

Case 4.1.a. $\theta_1^{(m)}$ is very close to λ_1.

Case 4.1.b. $\theta_1^{(m)}$ is between λ_1 and λ_2.

Case 4.1.c. $\theta_1^{(m)}$ is greater than λ_2.

In expressions (18) and (31), $\mathbf{R}_{m+j}$ is the block CG residual at $m+j$th step, and $\bar{\mathbf{R}}_j$ is the residual after j steps of block CG applied to $\bar{\mathbf{R}}_0 = (I - \Pi_Q)\mathbf{R}_m$. The counter m specifies the status of iteration advance of block CG when the bound starts to be employed. Hence, the evolution of m determines the status of convergence of θ_1 to λ_1 (see for instance Table 2), and the evolution of j determines the behavior of the bounds (see for instance Table 3).

Case 4.1.a. The first Ritz value θ_1 is very close to λ_1. Table 2 shows the behavior of $\alpha_{m,1,0}$ and γ_m at each iteration m. Bounds (18) and (24) computed with $j = 0$ are presented for several values of m. This computation shows how the main factors of both bounds α_{m,k_1,k_2} and γ_m behave in the final interval of convergence.

To simplify the notation, in this example, such bounds are denoted as b_1 and b_2 as follows:

$$b_1 = \|\bar{\mathbf{R}}_0\|_{A^{-1}\text{-}F} + \gamma_m \|\Pi_Q \mathbf{R}_m\|_{A^{-1}\text{-}F} \text{ and } b_2 = \alpha_{m,1,0}\|\bar{\mathbf{R}}_0\|_{A^{-1}\text{-}F}. \tag{36}$$

The comparison residual at iteration m is $\bar{\mathbf{R}}_0 = \|(I - \Pi_Q)\mathbf{R}_m\|_{A^{-1}\text{-}F}$. Observe that despite of the fact that the convergence of the Ritz vectors is slow and non-monotone [14], which has influence on γ_m, bound b_1 gives sharper estimates than b_2; see Table 2.

Table 2: Case 4.1.a. The first Ritz value $\theta_1^{(m)}$ is very close to smallest eigenvalue λ_1. Parameters $k_1 = 1$, $k_2 = 0$, $s = 1$ and $j = 0$. Factors γ_m and $\alpha_{m,1,0}$ are computed using (20) and (24), respectively. Bounds b_1 and b_2 correspond to (36).

m	θ_1	θ_1/λ_1	γ_m	$\alpha_{m,1,0}$	b_1	b_2	$\|\bar{\mathbf{R}}_0\|_{A^{-1}\text{-}F}$	$\|\mathbf{R}_m\|_{A^{-1}\text{-}F}$
30	0.12659	1.26597	0.61127	1.72469	0.77367	0.92530	0.53650	0.66210
31	0.12280	1.22800	0.56286	1.59067	0.67380	0.79217	0.49801	0.58784
32	0.11708	1.17082	0.48434	1.41203	0.53402	0.60523	0.42862	0.48069
33	0.11138	1.11386	0.39936	1.25698	0.39652	0.42922	0.34147	0.36825
34	0.10771	1.07712	0.33933	1.16715	0.29890	0.31279	0.26799	0.28305

It can also be observed that when m increases, then $\alpha_{m,1,0}$ decreases (ideally it tends to one) and γ_m also decreases (ideally tends to zero). Recall that when $\alpha_{m,1,0} = 1$ and $\gamma_m = 0$, then both bounds coincide. However, it can also be observed that bound b_2 is more sensitive to $\alpha_{m,1,0}$ than the bound b_1 to γ_m. This means that γ_m does not need to be close to zero in order to b_2 obtain a better approximation than b_1.

We examine now the long term behavior of both bounds but in the same stage of convergence of the Ritz values to their corresponding eigenvalues. To this end, we fix $m = 33$ and take iterations j from $j = 1$ to $j = 10$. To simplify the reading, the following notation is used

$$\begin{cases} b_{1,j} = \min_{\mathbf{D}\in A\mathbb{K}_j(A,\mathbf{R}_m)} \Big\{ \|(I - \Pi_Q)(\mathbf{R}_m - \mathbf{D})\|_{A^{-1}\text{-}F} \\ \qquad\qquad + \gamma_m \|\Pi_Q(\mathbf{R}_m - \mathbf{D})\|_{A^{-1}\text{-}F} \Big\} \qquad \text{and} \\ b_{2,j} = \alpha_{m,k_1,k_2}\|\bar{\mathbf{R}}_j\|_{A^{-1}\text{-}F}, \end{cases} \tag{37}$$

Table 3 shows the behavior of expressions $b_{1,j}$ and $b_{2,j}$, the residual of the comparison process $\|\bar{\mathbf{R}}_j\|_{A^{-1}\text{-}F}$ and the block CG residual $\|\mathbf{R}_{33+j}\|_{A^{-1}\text{-}F}$. It can be

Table 3: Case 4.1.a. The first Ritz value θ_1 very close to smallest eigenvalue λ_1. Parameters $k_1 = 1$, $k_2 = 0$, $s = 1$ and iteration $m = 33$. Factors $\alpha_{m,k_1,k_2} = \alpha_{33,1,0}$ and $\gamma_m = \gamma_{33}$ are computed using (24) and (20), respectively. Bounds $b_{1,j}$ and $b_{2,j}$ are given by (37).

θ_1	$\alpha_{33,1,0}$	γ_{33}	$\|\mathbf{R}_{33}\|_{A^{-1}\text{-}F}$
0.11138	1.25698	0.39936	0.36825

j	$b_{1,j}$	$b_{2,j}$	$\|\bar{\mathbf{R}}_j\|_{A^{-1}\text{-}F}$	$\|\mathbf{R}_{33+j}\|_{A^{-1}\text{-}F}$
1	0.34058	0.35903	0.28563	0.28305
2	0.29627	0.30365	0.24157	0.23350
3	0.27034	0.27142	0.21594	0.20939
4	0.25733	0.25542	0.20321	0.19836
5	0.25064	0.24739	0.19684	0.19279
6	0.24635	0.24246	0.19293	0.18896
7	0.24228	0.23803	0.18944	0.18476
8	0.23651	0.2320	0.18474	0.17775
9	0.22602	0.22135	0.17654	0.16362
10	0.20638	0.20139	0.16165	0.13714

observed that both $b_{1,j}$ and $b_{2,j}$ bound the optimal residual and the block CG residual in a similar manner.

It can also be observed that the norm block CG residual $\|\mathbf{R}_{33+j}\|_{A^{-1}\text{-}F}$ is smaller than the norm comparison residual $\|\bar{\mathbf{R}}_j\|_{A^{-1}\text{-}F}$. This is due to the fact that the comparison process $\|\bar{\mathbf{R}}_j\|_{A^{-1}\text{-}F}$ is built using a single eigenvalue ($k_1 = 1$ in this example), i.e., the comparison process is the residual with the eigenvalue λ_1 absent. Notice that the norm of the block CG residual is smaller than the norm of the comparison process. This implies that components corresponding to eigenvalues other than λ_1 are also absent in the block CG residual.

Case 4.1.b. The Ritz value θ_1 is between λ_1 and λ_2. Table 4 shows the results for some iterations ($m = 21, \ldots, 25$). In this interval the factor $\alpha_{m,1,0}$ suffers abrupt variations in comparison with γ_m. The variation of $\alpha_{m,1,0}$ is due to the proximity of $\theta_1^{(m)}$ to λ_2, which yields a very rough estimate by the bound b_2 of the block CG behavior. The estimate is improved either once $\theta_1^{(m)}$ moves away from λ_2 or by replacing the factor α_m by $\theta_1^{(m)}/\lambda_1$ as suggested in [23]. The latter results in a bound ($\frac{\theta_1}{\lambda_1}\|\bar{\mathbf{R}}_0\|_{A^{-1}\text{-}F}$) sharper than bound b_1 and b_2.

Table 4: Case 4.1.b. Ritz value θ_1 in $[\lambda_1, \lambda_2]$. Parameters $k_1 = 1$, $k_2 = 0$, $s = 1$, and $j = 0$. Factors $\alpha_{m,1,0}$ and γ_m are computed using (24) and (20), respectively. Bounds b_1 and b_2 correspond to (36).

m	$\theta_1^{(m)}$	θ_1/λ_1	γ_m	$\alpha_{m,1,0}$	b_1	b_2	$\|\bar{\mathbf{R}}_0\|_{A^{-1}\text{-}F}$	$\|\mathbf{R}_m\|_{A^{-1}\text{-}F}$
21	0.20181	2.0181	0.86898	110.93237	2.11922	113.62360	1.02426	1.62383
22	0.17786	1.7786	0.80929	8.0359	1.78204	6.28417	0.964314	1.39672
23	0.15595	1.5595	0.74794	3.5404	1.43954	2.47657	0.85200	1.15887
24	0.14271	1.4271	0.70553	2.4913	1.18655	1.59363	0.73686	0.97427
25	0.13622	1.3622	0.68186	2.1359	1.03745	1.29275	0.65704	0.86194

We consider next the $b_{1,j}$ and $b_{2,j}$ of expression (37) at the specific iteration $m = 23$, where $\theta_1^{(m)}$ fall almost exactly in the middle of $[\lambda_1, \lambda_2]$. Hence, the factor $\alpha_{m,1,0}$ is large and the bound $b_{2,j}$ overestimate the superlinearity. This can be observed in Table 5 which summaries these estimates for $\|\mathbf{R}_{23+j}\|_{A^{-1}\text{-}F}$ with $j = 1, \ldots, 10$. The bound $b_{2,j}$ is computed using the factor $\alpha_{m,1,0} = 3.54044$, which

Table 5: Case 4.1.b. Residual Bounds at $m = 23$, when θ_1 is in the middle of $[\lambda_1, \lambda_2]$. Parameters $k_1 = 1$, $k_2 = 0$ and $s = 1$. Factors $\alpha_{23,1,0}$ corresponds to (24) and γ_m to (20). Bounds b_1 and b_2 correspond to (37).

θ_1	$\alpha_{23,1,0}$	γ_{23}	$\|\mathbf{R}_{23}\|_{A^{-1}\text{-}F}$
0.15595	3.54044	0.74794	1.15887

j	$b_{1,j}$	$b_{2,j}$	$\|\bar{\mathbf{R}}_j\|_{A^{-1}\text{-}F}$	$\|\mathbf{R}_{23+j}\|_{A^{-1}\text{-}F}$
1	1.28592	2.47657	0.69950	0.97427
2	1.15295	2.01543	0.56925	0.86194
3	1.06385	1.71144	0.48339	0.80285
4	1.01284	1.54247	0.43567	0.77255
5	0.98455	1.45406	0.41070	0.75507
6	0.96687	1.40444	0.39668	0.74175
7	0.95238	1.36986	0.38691	0.72694
8	0.93562	1.33628	0.37743	0.70399
9	0.90988	1.29108	0.36466	0.66210
10	0.86496	1.21714	0.34378	0.58784

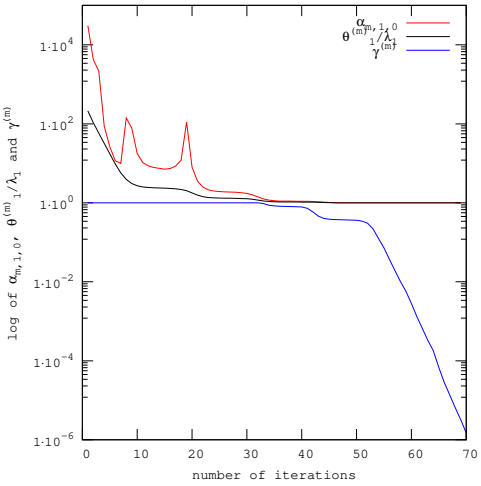

Fig. 2: Example 4.1 Case c. Behavior of $\alpha_{m,1,0}$ and γ_m of bounds b_1 and b_2 (expression (36)) correspond to the number of iterations m. The smallest Ritz value $\theta_1^{(m)}$ at mth iteration and smallest eigenvalue λ_1 of the matrix A.

has relatively moderate size in comparison with $\theta_1^{(m)}/\lambda_1$. It can be observed that $b_{1,j}$ is sharper than $b_{2,j}$ for all j.

Case 4.1.c. When $\theta_1^{(m)}$ is outside of its final interval of convergence. This happens when $m \leq 20$. In such a case, the factors $\alpha_{m,1,0}$ and γ_m have very different behavior; see Figure 2. As it can be observed, $\alpha_{m,1,0}$ has large variations when $\theta_1^{(m)}$ approaches a wrong eigenvalue, and consequently the bound computed with this factors did not provide any useful information. On the other hand, for $m \leq 20$ the value of γ_m remains almost equal to 1, that means that bound $b_{1,j}$ in equation (37) can be computed as $\|(I - \Pi_Q)\bar{\mathbf{R}}_j\|_{A^{-1}\text{-}F} + \|\Pi_Q \bar{\mathbf{R}}_j\|_{A^{-1}\text{-}F}$.

In summary, this example shows the behavior of the bounds in several stages of the convergence of the Ritz value $\theta_1^{(m)}$ towards the eigenvalue λ_1. It is observed

Table 6: Example 4.2. Ritz value $\theta_i^{(m)}$ for $i = 1, ..., 4$. The bounds area computed with $j = 0$, and parameters $k_1 = 4$ and $k_2 = 0$. Factors $\alpha_{m,4,0}$ corresponds to expression (32) and γ_m to expression (20). Bounds b_1 and b_2 correspond to expressions (36). The four smallest eigenvalues of this example are $\lambda_1 = 0.1, \lambda = 0.2, \lambda = 0.3$ and $\lambda = 0.4$.

m	$\theta_1^{(m)}$	$\theta_2^{(m)}$	$\theta_3^{(m)}$	$\theta_4^{(m)}$	$\alpha_{m,4,0}$	γ_m	b_1	b_2	$\|\bar{\mathbf{R}}_0\|_{A^{-1}\text{-}F}$	$\|\mathbf{R}_m\|_{A^{-1}\text{-}F}$
39	0.10485	0.24301	0.39061	5.00336	29249.6	0.99998	0.23883	1340.984	0.04584	0.19836
40	0.10469	0.24235	0.39033	4.99812	52236.3	0.99996	0.22012	1547.637	0.02962	0.19279
41	0.10458	0.24189	0.39013	4.98636	7124.5	0.99983	0.21305	184.532	0.02590	0.18896
42	0.10446	0.24138	0.38991	4.35890	131.885	0.98594	0.21336	4.53408	0.03437	0.18476
43	0.10426	0.24049	0.38949	2.33890	16.9294	0.95700	0.21476	0.88256	0.05213	0.17775
44	0.10384	0.23842	0.38838	1.10663	5.3865	0.88939	0.20429	0.40350	0.07491	0.16362
45	0.10302	0.23329	0.38414	0.58421	2.40210	0.75256	0.16799	0.16799	0.09033	0.13714
46	0.10185	0.22274	0.35799	0.42276	1.46327	0.55404	0.11397	0.12184	0.08327	0.10002

in **Case 4.1.a** that both bounds have similar results when the Ritz value has sufficiently converged to its corresponding eigenvalue. The **Case 4.1.b** (and **Case 4.1.c**) shows that the subspace bound is better than the spectral bound when the Ritz value $\theta_1^{(m)}$ is inside (or outside) its final interval of convergence but still far away of the corresponding eigenvalue λ_1.

Example 4.2. As mentioned at beginning of this section, the objective consists in to analyze the behavior of the bounds for capturing several eigenvalues simultaneously. To this end, in this example, we consider the four smallest eigenvalues in the construction of the bounds, i.e., $k_1 = 4$ and $k_2 = 0$. In this experiment, the initial iterate and matrix are the same as in the previous Example 4.1.

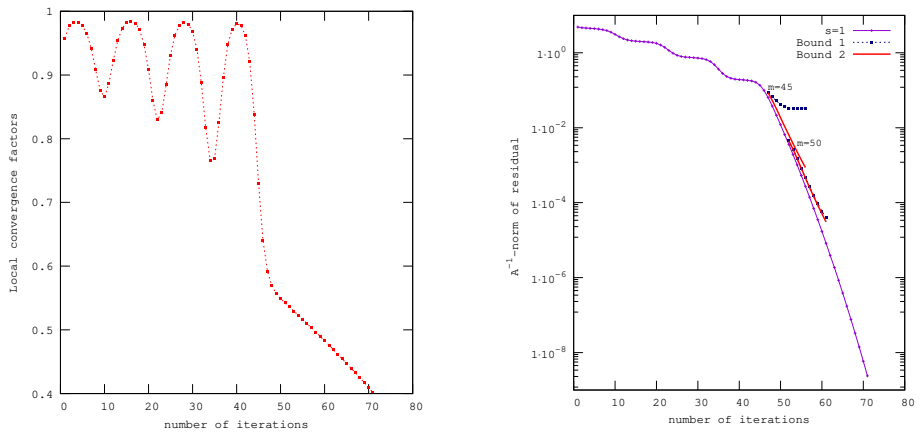

(a) (b)

Fig. 3: Example 4.2. (a) Local ratio of block CG residuals $\|\mathbf{R}_m\|_{A^{-1}}/\|\mathbf{R}_{m-1}\|_{A^{-1}}$. (b) Block CG residual $\|\mathbf{R}_m\|_{A^{-1}\text{-}F}$, Bound 1 and Bound 2 correspond to expressions (37) computed with $m = 45$ and $m = 50$. Parameters $k_1 = 4$ and $k_2 = 0$.

Table 6 shows the convergence of the Ritz values $\theta_i^{(m)}$ (for $i = 1, \ldots, 4$) to the four lowest eigenvalues and the behavior of $\alpha_{m,k_1,k_2} = \alpha_{m,4,0}$, and γ_m. In addition, we present bounds $b_{1,0}$ and $b_{2,0}$ given by expression (37), i.e., the bounds with $j = 0$; the comparison residual $\bar{\mathbf{R}}_0$, and the block CG residual $\mathbf{R}_m$. It is remarkable that the final superlinear phase begins when the four lowest Ritz values enter in its final interval

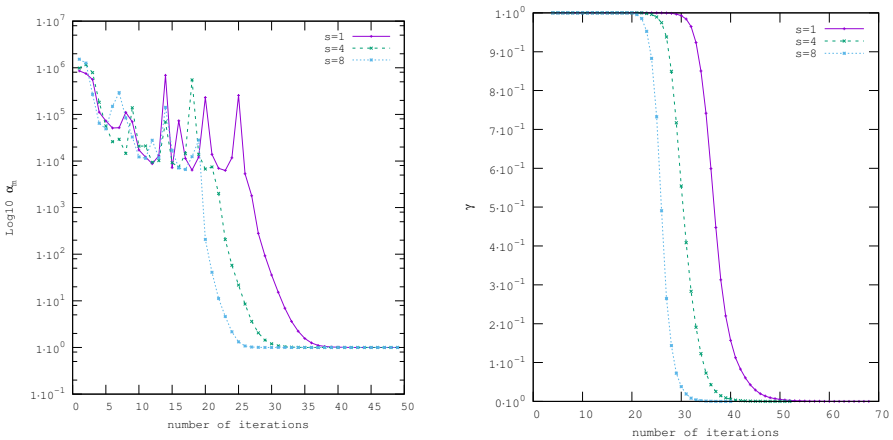

(a) Behavior of $\alpha_{m,1,0}$

(b) Behavior of γ_m

Fig. 4: Example 4.3. Behavior of $\alpha_{m,1,0}$ and γ_m correspond to the number of iterations m. $\alpha_{m,1,0}$ is computed with expression (32) and γ_m is computed with expression (20). Parameters $k_1 = 1$, $k_2 = 0$ and $s = 1, 4, 8$.

of convergence ($m \geq 40$). However, since $\theta_4^{(m)}$ is close to an eigenvalue different than λ_4, namely λ_5, the factor $\alpha_{m,4,0}$ suffers great variations.

To have a more complete picture of the superlinear behavior, in Table 6, we also present these factors $\alpha_{m,4,0}$, γ_m, and $\|\mathbf{R}_m\|_{A^{-1}\text{-}F}$ for larger values of m (from $m = 39$ to $m = 46$). From these iterations the Ritz values enter into their final intervals of convergence to their respective eigenvalues. The results are shown in Figure 3. Figure 3(a) shows the local ratios $\|\mathbf{R}_m\|_{A^{-1}\text{-}F}/\|\mathbf{R}_{m-1}\|_{A^{-1}\text{-}F}$ obtained during the CG process while Figure 3(b) shows the behavior of $\|\mathbf{R}_m\|_{A^{-1}\text{-}F}$ of the block CG, and the Bound 1 and Bound 2 as expressed in (37). It is observed that the local ratios $\|\mathbf{R}_m\|_{A^{-1}\text{-}F}/\|\mathbf{R}_{m-1}\|_{A^{-1}\text{-}F}$ decrease continuously, see Figure 3(a) implying a superlinear behavior; mainly after the 40th iteration ($m = 40$).

In Figure 3(b) it can be observed at the iteration $m = 45$ that the bound $b_{2,j}$ (spectral bound) is sharper than bound $b_{1,j}$ (subspace bound). This is because bound $b_{1,j}$ with a moderate γ_m ($\gamma_m = 0.75256$) amplifies significantly the residual component on the selected eigenspace $\mathbb{R}(Q)$. For iteration $m = 50$ the selected Ritz values are very close to its respective eigenvalues and the resulting bounds are almost the same, as it is expected.

Example 4.3. This example is designed to analyze the effect of the block size s on the bounds and on the convergence of the block CG in the presence of a single eigenvalue near the origin. This experiment considers a diagonal matrix of dimension 404×404 with eigenvalues on the diagonal with values $0.0005, 0.08, \ldots, 2.42$, that is, the matrix has one isolated eigenvalue near to zero and the other 403 eigenvalues are equally distributed between 0.08 and 2.42. It is expected to observe superlinear convergence once the method captures the lowest eigenvalue 0.005.

Figure 1 shows the convergence history for block sizes $s = 1$, 4 and 8. In this example, and in the following ones, when $s > 1$, the matrix $\mathbf{B}$ has repeated copies of b, but the initial set of vectors in $\mathbf{X}_0$ are nonzero and randomly generated, implying

that $\mathbf{R}_0$ has all distinct columns. On each residual history, we plot the two bounds $b_{1,j}$ and $b_{2,j}$ at different stages of convergence. For the computation of the bounds we used $k_1 = 1$ and $k_2 = 0$, i.e., in the comparison process the component of the error corresponding to the invariant subspace associated with the lowest eigenvalue is absent. Observe that for values of m relatively large, both bounds capture well the slope of the superlinear regime. In addition, observe that when the block size is increased, block CG hastens the onset of superlinear convergence, but going from $s = 4$ to $s = 8$ the difference in the onset is moderate.

Observe in Figure 1 that at the superlinear beginning (for earlier m) one can observe substantially different estimate bounds (the spectral bound $b_{2,j}$ is sharper than subspace bound $b_{1,j}$). This is due to the fact that factor γ_m has moderate values ($\gamma_m \in [0.5, 1]$)), introducing in expression $b_{1,j}$ a contribution from the invariant subspace $\mathbb{R}(Q)$. It is important to remark that moderate values of γ_m are in connection with the rate of convergence of Ritz vectors, which are slower than the convergence of the Ritz values. This can be appreciated by comparing Figures 4(a) and 4(b), that the convergence of $\alpha_{m,1,0}$ (to one) is faster than the convergence of γ_m (to zero).

In addition, in Figure 4(a), it can be observed the erratic convergence behavior of $\alpha_{m,1,0}$. In fact, it takes large oscillatory values before approaching the final interval of convergence of the Ritz values. On the other hand, the behavior of γ_m is smooth and well behaved (see Figure 4(b)). This indicates that the subspace bound $b_{1,j}$ is less sensitive to the stage of convergence of the Ritz value, hence it can be used safely to describe the behavior in this region.

Example 4.4. The objective of this example is to analyze the effect of the block size s on the convergence of block CG and the behavior of the bounds to capture the superlinearity in presence of a cluster of eigenvalues near the origin. To this end, in this example, we consider a diagonal matrix of dimension 404×404 with eigenvalues on the diagonal with values $0.0005, 0.0015, 0.0025, 0.0035, 0.0045, 0.0055, 0.08, \ldots, 2.42$. The matrix has six clustered eigenvalues near zero and the rest distributed uniformly between 0.08 and 2.42.

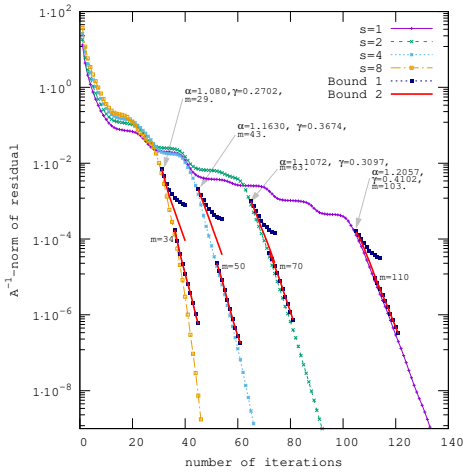

Fig. 5: Example 4.4. Residual convergence behavior for the block CG $\|\mathbf{R}_{m+j}\|_{A^{-1}\text{-}F}$ for $s = 1, 2, 4, 8$, Bound 1 and Bound 2 correspond to expressions (37). Parameters $k_1 = 6$ and $k_2 = 0$.

Figure 5 shows the convergence history of block CG, considering the invariant

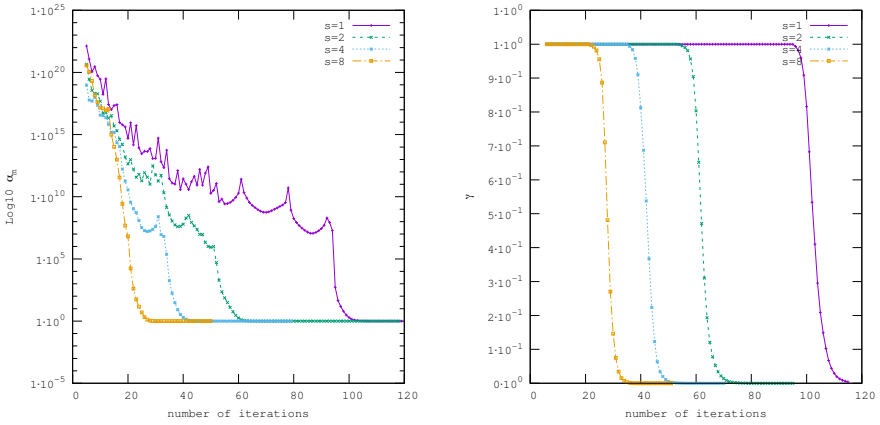

(a) Behavior of $\alpha_{m,6,0}$ correspond to m.

(b) Behavior of γ_m correspond to m.

Fig. 6: Example 4.4. Behavior of $\alpha_{m,6,0}$ and γ_m correspond to the number of iterations m. $\alpha_{m,6,0}$ is computed with expression (32) and γ_m is computed with expression (20). Parameters $k_1 = 6$, $k_2 = 0$ and $s = 1, 2, 4, 8$. (a) Behavior of $\alpha_{m,6,0}$ computed with expression (32), and (b) behavior of γ_m computed with expression (20).

subspace associated to the six lowest eigenvalues, i.e., both bounds are computed using $k_1 = 6$ and $k_2 = 0$ for each block size ($s = 1$, 2, 4 and 8). Contrasting the residual histories of the bounds (Figure 5) with the behavior of γ_m and $\alpha_{m,6,0}$ in Figure 6, one can observe that the superlinear behavior on the block CG begins when all Ritz values associated with the cluster eigenvalues enter its final interval of convergence. This is equivalent to the factor $\alpha_{m,6,0}$ be close to 1 or when γ_m is of moderate size ($\gamma_m \leq 0.5$), see Figure 6.

Observe in Figure 5 that when the block size is increased, the superlinear behavior starts earlier. This shows the dependency of the onset of the superlinear behavior on the block size. Moreover, this example suggests that block CG (with $s > 1$) hastens the onset of the superlinearity in the presence of clustered eigenvalues.

Example 4.5. In this example we analyze effect of an eigenvalue with algebraic multiplicity κ on the bounds $b_{1,j}$ and $b_{2,j}$. To this end, in this experiment we consider a 384×384 matrix with an eigenvalue $\lambda = 0.0005$ with algebraic multiplicity 5 in the lowest part of its spectrum. The rest of eigenvalues are uniformly distributed between 0.065 and 5.42.

Figure 7 shows the block CG residual, and bounds $b_{1,j}$ and $b_{2,j}$. When in the parameter k_1 equals the block size s (i.e., $k_1 = s$) (see Figures 7(a) and 7(c)) the spectral bound $b_{2,j}$ (defined in (37) with α_{m,k_1,k_2} introduced in Remark 7) approximates adequately the behavior of the residual. On the other hand, if k_1 is larger that the block size s (see Figures 7(b) and 7(d)), then the bound capture the slop but is not sharp. In all cases the subspace bound $b_{1,j}$ approximates adequately the behavior of the residual.

At this point, it is important to remark that the CG polynomial only captures one copy of the eigenvalue with multiplicity, but block CG can find up to s copies in the case of repeated eigenvalues [22]. This remark also applies for clustered eigenvalues. Hence, if $s = k_1 \leq \kappa$, block CG captures s eigenvalues and the spectral bound $b_{2,j}$ which uses these $k_1 = s$ eigenvalues approximates well the residual. However, if

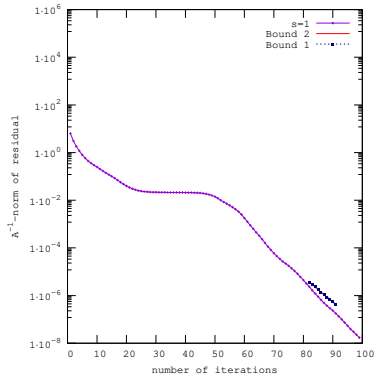

(a) $k_1 = 1$, $k_2 = 0$ and $s = 1$.

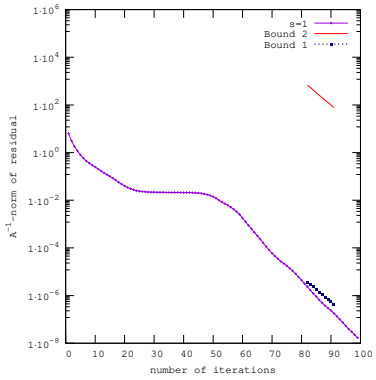

(b) $k_1 = 2$, $k_2 = 0$ and $s = 1$.

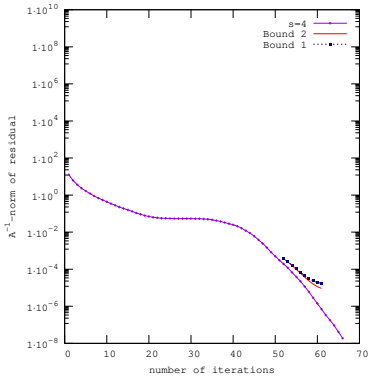

(c) $k_1 = 4$, $k_2 = 0$ and $s = 4$.

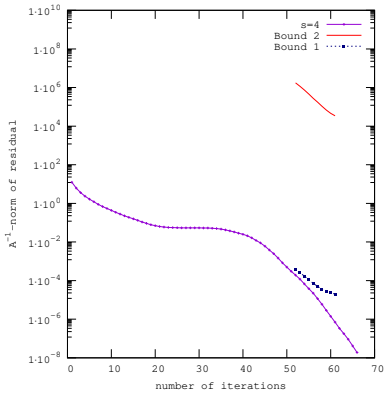

(d) $k_1 = 5$, $k_2 = 0$ and $s = 4$.

Fig. 7: Example 4.5. Residual convergence behavior for the block CG, Bound 1 and Bound 2 corresponding to expression (37) and $\left\|\bar{\mathbf{R}}_j\right\|_{A^{-1}\text{-}F}$. (a) Parameters values $s = k_1$ and $\alpha_{80,1,0} = 1.00002$, and (b) Parameters values $k_1 = 2$ and $\alpha_{80,2,0} = 1.83221 \times 10^8$. (c) Parameters values $s = k_1$ and $\alpha_{50,4,0} = 1.00108$, and (d) Parameters values $k_1 = 5$ and $\alpha_{50,5,0} = 4.718055 \times 10^9$.

$s < k_1 \leq \kappa$, then the bound is expected to capture more eigenvalues than the block CG is able to capture, and consequently the approximation bound is not sharp. Note the different horizontal scales in Figures 7(c) and (d) for $s = 4$, compared to that in Figures 7(a) and (b) for $s = 1$.

The analysis of this example suggest that when an eigenvalue with algebraic multiplicity κ is considered, the spectral-based bound approximates adequately the residual behavior when the number of eigenvalues taken as reference (denoted by $k_1 \leq \kappa$) is at most equal to the block size s.

In this example, it can also be observed that as the block size s is increased, the number of eigenvalues captured by block CG is larger, hence the onset of the superlinear convergence occurs earlier (compare for instance Figures 7(b) and 7(d). This is in accordance with the observation made in Example 4.4 showing a close relationship between block size s and the onset of superlinear convergence.

Example 4.6. In this example we consider a preconditioned 400×400 matrix from

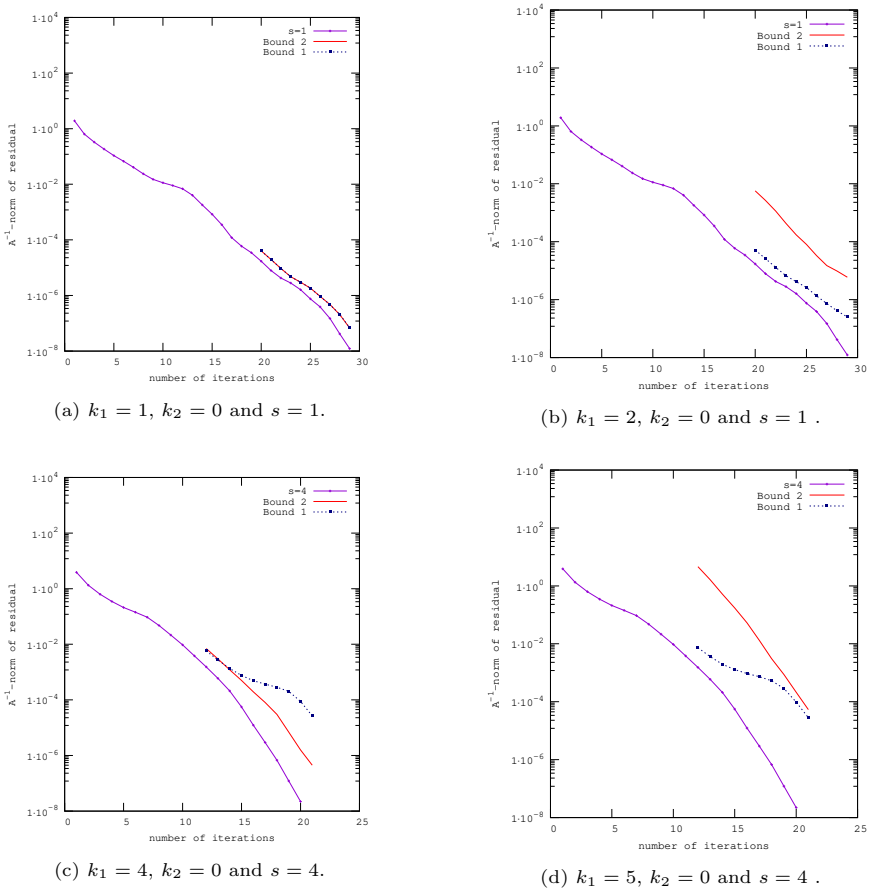

(a) $k_1 = 1$, $k_2 = 0$ and $s = 1$.

(b) $k_1 = 2$, $k_2 = 0$ and $s = 1$.

(c) $k_1 = 4$, $k_2 = 0$ and $s = 4$.

(d) $k_1 = 5$, $k_2 = 0$ and $s = 4$.

Fig. 8: Example 4.6. Poisson matrix preconditioned using an incomplete Cholesky factorization. Residual convergence behavior for the block CG, the bound $b_{2,j}$ corresponding to expression (37) and $\|\tilde{\mathbf{R}}_j\|_{A^{-1}\text{-}F}$. (a) Parameters $k_1 = 1$ and $\alpha_{20,1,0} = 1.01$. (b) Parameters $k_1 = 2$ and $\alpha_{20,2,0} = 89.4478$. (c) Parameters $k_1 = 4$ and $\alpha_{10,4,0} = 1.448558$. (d) Parameters $k_1 = 7$ and $\alpha_{10,7,0} = 29.224$.

a discrete 2D Poisson equation. The incomplete Cholesky factorization with no fill is used as preconditioner, i.e., the coefficient matrix is $\tilde{A} = L^{-1}AL^{-T}$. The maximum eigenvalue is 1.2015 and the minimum is 0.0724. The ten smallest eigenvalues are 0.0724, 0.1652, 0.1699, 0.2483, 0.2971, 0.2994, 0.3486, 0.3742, 0.4362, 0.4367, 0.4396, 0.4802. The rest of the eigenvalues are distributed between 0.5014 and 1.2015.

Figure 8 shows the behavior of the residual and its approximation using bounds $b_{1,j}$ and $b_{2,j}$ introduced in (37) with block size $s = 1$, and parameters values k_1 and k_2 in two situations: (a) $k_1 = 1$ and $k_2 = 0$, and (b) $k_1 = 2$ and $k_2 = 0$. Figure 8(a) shows a good approximation of the bound to the block CG residual. This is in accordance with the observation made that the convergence is mainly due to the convergence of the first eigenvalue. It can also be observed (similar to Example 4.5) that when k_1 is larger than s, the bounds capture the slope of the residual but the spectral bound $b_{2,j}$ is not sharp (see Figure 8(b)). Similar observation can be done for a larger block sizes, for instance, Figures 8(c) and 8(d) for values of $k_1 = 4$, $k_2 = 0$ and $s = 4$, and $k_1 = 5$, $k_2 = 0$ and $s = 5$, respectively.

Finally, comparing Figures 8(c) and 8(d), since more eigenvalues are captured when the block size is increased, the onset of the superlinear convergence occurs earlier. Again, note the different horizontal scale of these two figures for $s = 4$ as compared to those with $s = 1$.

5. Conclusions. In this article, we have extended the *a posteriori* spectral bound introduced by van der Sluis and van der Vorst [23] to the block CG case. We have also implemented the subspace bound introduced previously by Simoncini and Szyld [17]. Example experiments show that both bounds capture the slope of the residual in the superlinear phase of the convergence of the block CG method. In addition, when there is a cluster of eigenvalues in the lower part of the matrix spectrum, the spectral bound captures better the superlinearity even at the initial stages, while the subspace bound captures better the superlinearity in presence of repeated eigenvalues.

Analyzing the bounds and the residual behavior of the block CG method, it is observed that the block method accelerates the convergence because it captures more eigenvalues. Therefore, in the presence of a cluster or repeated eigenvalues in the lower part of the spectrum, the larger is the block size s, the earlier is the onset of the superlinear convergence. Hence in these cases we suggest the use of block CG with the block size of the order of to the size of the cluster.

REFERENCES

[1] B. Beckermann and A. B. Kuijlaars, *Superlinear convergence of conjugate gradients*, SIAM Journal on Numerical Analysis, 39 (2001), pp. 300–329, http://dx.doi.org/10.1137/S0036142999363188.

[2] B. Beckermann and A. B. Kuijlaars, *Superlinear CG convergence for special right-hand sides*, Electronic Transactions on Numerical Analysis, 14 (2002), pp. 1–19.

[3] A. El Guennouni, K. Jbilou, and H. Sadok, *The block Lanczos method for linear systems with multiple right-hand sides*, Applied Numerical Mathematics, 51 (2004), pp. 243 – 256.

[4] A. Frommer, K. Lund, and D. B. Szyld, *Block Krylov subspace methods for functions of matrices*, Electronic Transactions on Numerical Analysis, 47 (2017), pp. 100–126.

[5] A. Frommer, K. Lund, and D. B. Szyld, *Block Krylov subspace methods for functions of matrices II: Modified block FOM*, SIAM Journal on Matrix Analysis and Applications, 41 (2020), pp. 804–837.

[6] G. H. Golub and C. F. Van Loan, *Matrix Computations*, The Johns Hopkins University Press, Baltimore, 4th ed., 2013.

[7] A. Greenbaum, *Iterative methods for solving linear systems*, SIAM, Philadelphia, 1997.

[8] M. H. Gutknecht, *Block Krylov space methods for linear systems with multiple right-hand sides: An introduction*, in Modern Mathematical Models, Methods and Algorithms for Real World Systems, A. Siddiqi, I. Duff, and O. Christensen, eds., Anamaya, New Delhi, 2007, pp. 420–447.

[9] M. H. Gutknecht and T. Schmelzer, *The block grade of a block Krylov space*, Linear Algebra and its Applications, 430 (2009), pp. 174 – 185, doi:http://dx.doi.org/10.1016/j.laa.2008.07.008.

[10] M. R. Hestenes and E. Stiefel, *Methods of conjugate gradients for solving linear systems*, Journal of Research of the National Bureau of Standards, 49 (1952).

[11] T. Kato, *Perturbation theory for linear operators*, Springer, Berlin, 2013.

[12] M. D. Kent, *Chebyshev, Krylov, Lanczos: Matrix Relationship and Computations*, PhD thesis, Department of Computer Science - Stanford University, 1989.

[13] D. P. O'Leary, *The block conjugate gradient algorithm and related methods*, Linear Algebra and its Applications, 29 (1980), pp. 293–322.

[14] Y. Saad, *On the Rates of Convergence of the Lanczos and the Block-Lanczos Methods*, SIAM Journal on Numerical Analysis, 17 (1980), pp. 687–706, doi:10.1137/0717059.

[15] Y. Saad, *Iterative methods for sparse linear systems*, vol. 82, SIAM, Philadelphia, 2003.

[16] V. Simoncini, *Ritz and Pseudo-Ritz values using matrix polynomials*, Linear Algebra and its Applications, 241 (1996), pp. 787 – 801, doi:http://dx.doi.org/10.1016/0024-3795(95)

00682-6.

[17] V. Simoncini and D. B. Szyld, *On the occurrence of superlinear convergence of exact and inexact Krylov subspace methods*, SIAM Review, 47 (2005), pp. 247–272, http://dx.doi.org/10.1137/S0036144503424439.

[18] V. Simoncini and D. B. Szyld, *Recent computational developments in Krylov subspace methods for linear systems*, Numerical Linear Algebra with Applications, 14 (2007), pp. 1–59.

[19] V. Simoncini and D. B. Szyld, *On the superlinear convergence of MINRES*, in Numerical Mathematics and Advanced Applications 2011 - Proceedings of ENUMATH 2011, the 9th European Conference on Numerical Mathematics and Advanced Applications, Leicester, September 2011, Berlin and Heidelberg, 2013, Springer, pp. 733–740.

[20] G. Sleijpen and A. van der Sluis, *Further results on the convergence behavior of conjugate-gradients and Ritz values*, Linear Algebra and its Applications, 246 (1996), pp. 233 – 278, doi:https://doi.org/10.1016/0024-3795(94)00360-2.

[21] G. W. Stewart and J.-G. Sun, *Matrix Perturbation Theory*, Academic Press, London, 1990.

[22] R. Underwood, *An iterative block Lanczos method for the solution of large sparse symmetric eigenproblems*, PhD thesis, Department of Computer Science, Tech Rept. 496, Stanford University, 1975.

[23] A. van der Sluis and H. A. van der Vorst, *The rate of convergence of Conjugate Gradients*, Numerische Mathematik, 48 (1986), pp. 543–560, http://dx.doi.org/10.1007/BF01389450.

[24] A. van der Sluis and H. A. van der Vorst, *The convergence behavior of Ritz values in the presence of close eigenvalues*, Linear Algebra and its Applications, 88 (1987), pp. 651–694.

[25] H. A. van der Vorst and C. Vuik, *The superlinear convergence behaviour of GMRES*, Journal of Computational and Applied Mathematics, 48 (1993), pp. 327 – 341, doi:http://dx.doi.org/10.1016/0377-0427(93)90028-A.